Echinacea angustifolia encapsulated with alginate/chitosan nanoparticles as a novel candidate carrier for combating multidrug-resistant Staphylococcus aureus

Sepideh Taghiloo
Islamic Azad University
Tohid Piri-Gharaghie (Tohid.piri71@gmail.com)
BIO3P company of AmitisGen Med TECH Group
Zahra Zand
Tehran Medical Sciences, Islamic Azad University
Saber Kabiri-Samani
Islamic Azad University
Hamidreza Kabiri
Islamic Azad University
Negin Rajaei
Islamic Azad University

Research Article

Keywords: Echinacea angustifolia, Drug delivery, Chitosan, Antibacterial activity, Alginate

Posted Date: October 18th, 2022

DOI: https://doi.org/10.21203/rs.3.rs-2163534/v1

Abstract

Background and aim:

The urgent need for breakthrough therapeutic approaches for multi-drug resistance *Staphylococcus aureus* (MDR) has drawn attention to potential cutting-edge tools like nanoparticles (NPs). The preparation of chitosan/alginate-encapsulated *Echinacea angustifolia* extract and evaluation of its effectiveness against MDR strains were the goals of this investigation.

Method

Scanning electron microscopy, dynamic light scattering (DLS), and Fourier Transform Infrared spectroscopy were used to analyze the synthesized NPs. Investigations were done into the antibacterial and antibiofilm properties of *E. angustifolia* NPs. Also, the expression of essential genes in biofilm formation was evaluated by real-time PCR.

Results

According to DLS measurements, spherical *E. angustifolia* NPs had a diameter of 335.3 ± 1.43 nm. The PDI was 0.681, and the entrapment effectiveness (EE%) of the *E. angustifolia* extract reached 83.45%. Synthesized NPs had the highest antibacterial power. They also significantly decreased the expression of genes involved in biofilm formation.

Conclusion

By releasing natural-derived medications under regulated conditions, the findings described here should help create new plant extracts with increased stability and antibacterial action, which will help minimize the usage of antibiotics.

1. Introduction

Bacterial infections are one of the most critical global health problems due to their high rates of morbidity and mortality, as well as the frequent introduction of antibiotic-resistant bacteria (Scolari et al., 2020). As a result, it is urgently necessary to create novel tactics that effectively combat infections (Roca et al., 2015). One opportunistic pathogen responsible for nosocomial diseases and serious illnesses is *Staphylococcus aureus* (Mirzaie et al., 2020). These bacteria cause many ailments, including food poisoning and potentially fatal conditions, including endocarditis and toxic shock syndrome (Bajaj et al., 2020). It exhibits a wide range of antibiotic resistance, including resistance to methicillin and vancomycin, which causes it to develop into methicillin-resistant *S. aureus* (MRSA) strains (Assis et al., 2017). Staphylococcal infections have become a significant independent problem with the appearance of MRSA (Kumar., 2020). The treatment of *S. aureus* infections may be limited since a large portion of MRSA strains are resistant to numerous antimicrobial drugs (Kumar., 2020). Additionally, one of the primary causes of the emergence of multidrug-resistant (MDR) *S. aureus* is the production of biofilms (Dey et al., 2019). Numerous clinical diseases, such as skin infections, pneumonia, meningitis, osteomyelitis, endocarditis, and sepsis, have been documented to be complicated by biofilm development (Mahmoudi et al., 2019). A biofilm is a multilayered, organized population of bacteria that can adhere to live surfaces and is protected by an exopolysaccharide glycocalyx (Mahmoudi et al., 2019). Numerous researches have examined the relationship between biofilm and antibiotic resistance in *S. aureus* and found that bacteria within the biofilm are kept secure and develop further antibiotic resistance (Banerjee et al., 2020).

Over time, scientists have developed and experimented with nanoparticles made of lipids, polysaccharides, and biopolymers, both synthetic and natural (Li et al., 2008). The concept of employing medication delivery nanoparticles produced from organic, biodegradable polymers has recently sparked a lot of attention (Jacob et al., 2018). Alginate (ALG) and chitosan (CS) are among them and have been extensively used in the pharmaceutical business for regulating medication release (Gombotz et al., 1998). ALG is a brown seaweed-derived water-soluble linear polysaccharide that is made up of alternating blocks of 1–4 linked -L-guluronic and -D-mannuronic acid residues (Smidsrød et al., 1990). Recently, CS was selected as a substitute for cationic

polymers that formed polysaccharides made of glucosamine and N-acetylglucosamine units (Pan et al., 2002). According to reports, ALG and CS are mucoadhesive, biodegradable, and biocompatible, and they have the potential for a wide range of therapeutic purposes, including cell encapsulation and drug delivery systems (Bhunchu et al., 2014). Additionally, alginate-chitosan nanoparticles may be produced utilizing a safe and straightforward process, such as polyelectrolyte complexation and ionic gelation, without the use of any dangerous chemicals that can impair an agent's functionality or integrity (Kaur et al., 2020).

Due to the increased incidence of bacteria that are resistant to antibiotics, which is exceedingly harmful to individuals and onerous for society, alternatives to standard antibiotics are crucial. An example of such candidates is herbal medicine, which also exhibits additional benefits like minor side effects and antibacterial properties (Sharifi-Rad et al., 2018). Natural healer *Echinacea Angustifolia* has been used for centuries to cure a variety of illnesses, including the common cold and cough, toothaches, stomach discomfort, and skin infections (Sharifi-Rad et al., 2018). Essential chemical elements of *Echinacea* species include volatile terpenes such as germacrene D, polyacetylenes, highly unsaturated alkamides, phenolic compounds, and glycoproteins, in addition to the presence of high molecular weight polysaccharides (Mistrikova et al., 2006). Previous research has shown that encapsulating *E. angustifolia* extract with nanoparticles can increase its antimicrobial properties (Sharifi-Rad et al., 2018).

Additionally, it has been demonstrated that nanoparticles (NPs) made from the combination of these two natural polymers have higher physical durability than NPs made from either polymer alone (Di Martino et al., 2018; Lertsutthiwong et al., 2009). But what makes this study unique is that it is the first to demonstrate the encapsulation of *E. angustifolia* within biodegradable polymeric ALG and CS. For this reason, in this work, an effort was made to encapsulate *E. angustifolia* in its active state within alginate-chitosan nanoparticles to increase their stability, curative impact, and prolonged release. The efficacy of encapsulation, release profile, particle size, and stability characteristics were evaluated and adjusted in the formulations of the encapsulated *E. angustifolia* extract. Additionally, against MRSA biofilm-forming clinical strains, the antibacterial and biofilm inhibitory potencies of optimized nanoparticles containing *E. angustifolia* were examined.

2. Materials And Methods

2.1. Materials

Medium-weight chitosan (75% deacetylation) and sodium alginate (medium viscosity) were bought from Sigma Aldrich in the United States. We purchased a dialysis membrane from Merck (MWCO 12,000 Da) (Darmstadt, Germany). RNA extraction and cDNA synthesis kits were purchased from Sinaclon (Iran, Tehran). The standard strain of *Staphylococcus aureus* ATCCBAA 33592 (MRSA) from the Iranian Biological Resource Center. Gibco provided the necessary supplies for cell culture, such as RPMI-1640, 3-[4,5-Dimethyl-2-thiazolyl]-2,5-diphenyl tetrazolium bromide (MTT), and PBS (phosphate-buffered saline) (Grand Island, NY, USA).

2.2. Plant material extraction

E. angustifolia was received from the plant bank of the Center for Biological Resources of Iran, and the botanical department approved its use for study. *E. angustifolia* aerial portions that had been dried and finely powdered (10 g) was dissolved in 100 ml of methanol in a Soxhlet extractor for two days. Rotary evaporators (Heidolph, Germany) were then used to evaporate the solvent. The resultant solid powder was twice cleaned with distilled water and stored at four °C until it was utilized to create ALG-CS NPs (Ghajari et al., 2021).

2.3. Encapsulation of E. angustifolia

By emulsifying both biopolymers and then electrostatically gelating them as per an adapted approach, *E. angustifolia* extract was encapsulated in CS-ALG nanoparticles. The *E. angustifolia* NPs were synthesized, in summary, by an ionic gelation process. To create the *E. angustifolia*-loaded ALG NPs, the *E. angustifolia* extract was first mixed in a 0.16% w/v T80 aqueous solution and added to the ALG aqueous solution (0.06% w/v, pH 5.5). This was done while stirring at 300 rpm and at room temperature. To create the *E. angustifolia* -loaded ALG NPs, an additional 0.05% w/v CaCl2 aqueous solution was added after that. Next, a

0.05% w/v CS in 1% v/v acetic acid aqueous solution (pH 4.5) was added to *the E. angustifolia*-loaded ALG NPs produced in the preceding procedure (Piri-Gharaghie et al., 2022). ALG/CS nanoparticles with *E. angustifolia* loaded on them were created using the formula presented at Table 1.

Table 1
Designed formulation of ALG/CS-encapsulated *E. angustifolia.*

Formulations	Different compounds	molar ratio	Drug concentration (g/ml)
F1	Chitosan + Alginate	1:1	1
F2	*E. angustifolia*	---	1
F3	*E. angustifolia* + alginate + chitosan	1:(0.5 + 0.5)	1

Table 2
The sequence of the specific primers used in qRT-PCR gene expression investigation.

Gene name	Sequence 5 ' to 3.'	Product size
IcaA	F: CAATACTATTTCGGGTGTCTTCACTCT	102 bp
	R: CAAGAAACTGCAATATCTTCGGTAATCAT	
IcaD	F: TCAAGCCCAGACAGAGGGAATA	83 bp
	R: ACACGATATAGCGATAAGTGCTGTTT	
pgaB	F: AGAACCTACAACTTCAGAACCTGTG	120 bp
	ACCCTTTAACCGTAGTTGGCGGTAT	
16S r-RNA	F- GCTGCCCTTTGTATTGTC	179 bp
	R-AGATGTTGGGTTAAGTCCC	

2.4. Characterization of nanoparticles

2.4.1. The polydispersity index (PDI), FTIR, size, and morphology

E. angustifolia-ALG-CS particle size and charge were determined using dynamic light scattering (DLS) and palladium electrodes of the ZetaPals device (Brookhaven Instruments Corp., USA) at a light scattering angle of 90° and a temperature of 25°C. Field scanning electron microscopy (FESEM) model MIRA3 (TESCAN, Czech Republic) was used to examine the topology of *E. angustifolia*-ALG-CS NPs. Fourier transform infrared spectroscopy was used to investigate the molecular interaction between *E. angustifolia* extract and ALG-CS (FTIR, TENSOR II, BRUKER, Germany). The dry potassium bromide (KBr) was combined with the dry nanoparticles, which were each weighed at around 2 mg. A tablet press created a uniform sheet. The resolution was set to 2 $cm^{-}1$, and the wavenumber range was 400–4000 $cm^{-}1$ (Mahmoudi et al., 2019; Sohrabi et al., 2016).

2.4.2. Efficacy of E. angustifolia encapsulation

Encapsulation efficiency (EE%) was assessed following the encapsulation of *E. angustifolia* in ALG-CS nanogels. An ordinary technique involved centrifuging 1 mL of *E. angustifolia*-loaded ALG-CS for 1 hour at 14000 g at four °C. UV-vis spectroscopy was used to determine the concentration of *E. angustifolia* in the supernatant at the drug's maximum-wavelength absorbance peak (334 nm) (Rinaldi et al., 2019). It is possible to identify the EE by:

$$EE\% = \frac{(T-F)}{T} \times 100$$

Where F stands for the amount of drug that is free in the supernatant and T for the overall amount of medicine. Using a blank sample.

2.4.3.Research on in vitro release

For research on in vitro drug release, a dialysis bag was employed. To do this, 2 mL of free *E. angustifolia* and 2 mL of *E. angustifolia* -ALG-CS were added to the dialysis bag. The whole fraction was then added to 50 mL of PBS solution with pHs of 3, 5, and 7.4 and slowly stirred at 37°C and 50 rpm. Sampling was done at various time intervals and replaced with new PBS. Additionally, the free *E. angustifolia* was subjected to the same process (Shukla et al., 2019).

2.5. The synthesized NPs' bioactivity

2.5.1. Sampling and bacterial strain isolation

100 clinical samples from several hospitals in Iran, including Nikan, Shohadaye Tajrish Hospital, and Sasan, containing blood, wound pus, sputum, urine, and more, were gathered for this research work between the years 2020 and 2021. The isolated samples were grown in blood agar, TSB, MacConkey, and Simmons citrate agar cultures at 37°C for 24 hours. Gram staining, catalase, oxidase, urease, and lysine decarboxylase tests all verified the detection of Staphylococcus aureus isolates. Additionally, the Kirby-Bauer disc diffusion method, based on the CLSI (Clinical and Laboratory Standards Institute, 2019) protocol, was used to evaluate antibiotic susceptibility (Banoub et al., 2021). Muller Hinton agar culture was used to assess the sensitivity of *Staphylococcus aureus* isolates to imipenem (IMI, 10 g), methicillin (MET, 10 g), ciprofloxacin (CIP, 5 g), vancomycin (VA, 10 g), erythromycin (E, 15 g), chloramphenicol (C, 30 g), amikacin (AK, 10), clindamycin (CD, 2 µg), kanamycin (KAN, 30 µg), ceftazidime (CAZ, 30 µg) and colistin (CS, 5 µg) and), tetracycline (TE, 30 µg) (MAST, UK) disks. The selection of multidrug-resistant (MDR) isolates was determined by the presence of at least one antibiotic resistance. The positive control organisms include Staphylococcus aureus ATCCBAA 33592, Pseudomonas ATCC 27853, and Acinetobacter ATCC 17978.

2.5.2. Evaluation of biofilm formation

The Mariana et al. approach was used to detect the generation of biofilm (Mariana et al., 2009). In a nutshell, bacterial culture was grown overnight at 37°C in congo red agar (CRA) plates supplemented with glucose (50 g/L), agar (10 g/L), congo red (0.08%), and BHIA with sucrose (37 g/L). A plate microtiter test was used to assess the isolates' ability to generate biofilms. In this test, isolated bacteria were first incubated, and then 200 µl of bacterial suspension was put into each well of a sterile 96-well polystyrene plate. The bacteria were then incubated for 24 hours at 37 ºC. 200 µl of crystal violet dye (1% concentration) was applied for staining, and after 15 minutes, it was rinsed with phosphate-buffered saline (PBS). OD570 was assessed using an ELISA Reader Stat Fax2100 (Awareness Technology, Ukraine) following the addition of 200 µl of acetic acid (33%). The results of the biofilm formation were categorized into the following groups:

- Non-biofilm producer: $OD \leq ODc$
- Weak biofilm producer: $ODc < OD \leq 2*ODc$
- Moderate biofilm producer: $2*ODc < OD \leq 4*ODc$
- Strong biofilm producer: $4*ODc < OD$

2.6. Evaluation of the antibacterial and anti-biofilm activity of E. angustifolia ALD-CS NPs

2.6.1. Minimum inhibitory concentration (MIC) and minimum bactericidal concentration (MBC)

Using broth microdilution technique in accordance with CLSI standards (2019), the formulations listed in Table 1 were tested to determine their minimum inhibitory concentration (MIC) and minimum bactericidal concentration (MBC). By diluting the free and encapsulated extract with Müller-Hinton Broth, various concentrations, ranging from 0, 0.5, 1.0, 2, 4, 8, 16, 32, 64, 128, 256 µg/mL-1, were achieved (MHB). A 96-well plate was first filled with 200 µl of each concentration, then 80 µl of MHB and 20 µl of microbial suspension at a concentration of 5×10^5 colony forming units (CFU) were added. After 24 h of incubation at 37°C, the MIC and MBC values were then calculated. The sub-MIC values of the positive control well, which included culture media plus the

standard *Staphylococcus aureus* strain ATCC 33592, and the negative control well, which contained pure culture medium, were determined, and the test was repeated (Targhi et al., 2021).

2.6.2. Agar well diffusion method

Agar well diffusion was used to test the antibacterial activity of the ALG/CS-encapsulated nanoparticles. Briefly stated, the bacteria were cultivated on nutrient broth (Condalab, Madrid) at 37°C overnight. A standard inoculum of each bacterial isolate was generated after incubation at a concentration of 1.5×10^8 CFU/mL in sterile normal saline and compared with a 0.5 McFarland standard solution. To evenly distribute bacteria throughout the surface of the plate, a sterile swab was dipped into the solution and then inoculated on a Muller-Hinton agar (Condalab, Madrid) plate. Using sterile cork borers, wells with a diameter of 6 mm were drilled into the medium, and 100 µL of sub-MIC concentration of the free NPs, free extract, and capsuled *E. angustifolia* were added to each well. After that, the plates were incubated for 24 hours at 37°C. After incubation, the inhibition zones around the wells were measured in millimeters to evaluate the antimicrobial activities. Water was regarded as a negative control.

2.6.3. Anti-Biofilm Activity

The 4 *S. aureus* strains that make up the biofilm (Sample 8, Sample 12, Sample 13, and Sample 22) and standard *S. aureus* ATCC 33592 were tested against sub-MIC concentrations of free *E. angustifolia* extract and ALG-CS-encapsulated *E. angustifolia* to determine the Minimum Biofilm Inhibition Concentration (MBIC). A 100 µl NPs sample and a 100 µl culture of bacteria in Müller Hinton Broth were placed in each of the 96 wells of the plate. The plates were rinsed, then dyed with violet crystal, and incubated for 48 hours at 37°C (Tan et al., 2018).

2.6.4. Quantitative real-time PCR for pgaB, IcaA, and IcaD expression detection

The polymerase chain reaction was used to examine the expression of the biofilm genes *IcaD*, *IcaA*, and *IcaC* using the particular primers specified in Table 1. Using the RNA extraction kit, RNA was extracted from multi-resistant *S. aureus* bacteria after 24 hours of exposure to a sub-MIC concentration of free *E. angustifolia* and ALG-CS-encapsulated *E. angustifolia*. cDNA was synthesized from the extracted RNA according to the instructions of the Sinaclone kit. With a total volume of 15 µl, quantitative real-time PCR was performed using 8 µl of PoweUpTM SYBR Green/ROX PCR Master Mix (Applied Biosystems, ThermoFisher Scientific, USA), 2 µl of forward and reverse primers, 1 µl of cDNA, and 4 µl of deionized water (Merck, Germany). The qPCR settings included a 15-minute initial denaturation step at 95°C, 40 cycles of denaturation (95°C for 30 s), annealing (58°C for 20 s), extension (72°C for 20 s), and melting curve analysis (60°C to 95°C). The $2^{-\Delta\Delta ct}$ technique was used to examine the relative gene expression. 16Sr-RNA served as the reference gene (El-Far et al., 2021).

2.7. Cytotoxicity study

Using the MTT test, the cytotoxicity of CS/ALG, free, and encapsulated *E. angustifolia* extracts was assessed against the human embryonic kidney (HEK 293) normal cell line. $5 - 2 \times 10^4$ cells were first seeded on a 96-well plate and exposed to various concentrations of samples (1-250µmol/ml) for 24 hours at 37°C with 5% CO2. After that, 100 µl of MTT [(3-(4, 5-dimethylthiazol-2-yl)-2, 5- diphenyl-tetrazolium bromide] dye (0.5 mg/ml) was added to the wells, and incubation was carried out for an additional 4 hours at 37 ºC. After removing the supernatant, 100 µl of DMSO (dimethyl sulfoxide) was added, and the mixture was shaken for 5 minutes. Finally, an ELISA plate reader reading the wells' optical density at 570 nm was used to determine the cell survival rate using the formula. The lethal dosage was chosen at 30% or a cytotoxic cut-off of 70% viable cells.

Cell viability % = (OD570 sample/OD570control) × 100

2.8. Statistical analysis

Each result was provided as Mean ± SD after the data were statistically evaluated using the GraphPad Prism 5.0 tool. To analyze the data, a one-way analysis of variance was employed (ANOVA). To compare groups in pairs, a T-test analysis with a 0.05 p-value was utilized.

3. Results

3.1. Fourier Transform Infrared Spectrometry (FTIR)

The FTIR spectra of the free extract, free NPs, and *E. angustifolia*-loaded ALG/CS nanoparticles are displayed in Fig. 1. The primary characteristic peaks of the generated free ALG/CS nanoparticles were found at 1098, 1639, 2926, and 3435 cm^{-1}, respectively, for the amino group (C-N), carboxylate group (COO), secondary amine (NH2), and the amine and hydroxyl groups stretch (N-H and O-H) (Fig. 1B). Furthermore, the main characteristic spectra for the amino group (C-N) and the CH2 bend, carboxylate group (COO), secondary amine group (NH2), and amine and hydroxyl (N-H and O-H) stretch were found at 1088, 1639, 2426, and 3435 cm^{-1}, respectively, in the synthesized *E. angustifolia*-loaded ALG/CS NPs (Fig. 1C). Figure 1A shows a wide band at 34535cm^{-1} that was attributed to the O-H stretching vibration in *E. angustifolia*. Accordingly, after complexation, the peak absorbance of the amino groups, carboxyl groups, secondary amine groups, and the amine and hydroxyl stretching vibrations changed somewhat in the ALG/CS NPs and the ALG/CS NPs that were also loaded with *E. angustifolia*. These findings suggest that electrostatic attraction enabled the carboxylate group of the ALG to engage with the amino group of protonated CS. Additionally, the hydroxyl group stretch and the symmetric hydrocarbon band in the *E. angustifolia*-loaded ALG-CS nanoparticles showed little change. These band changes demonstrate that the nanoparticle complex and *E. angustifolia* interact.

3.2. Characterization of E. angustifolia-ALG/CS NPs

Using SEM, the nanoparticles' surface morphology was investigated. Figures 2A and 2B correspondingly demonstrate the SEM images for the free and *E. angustifolia* -loaded ALG/CS nanoparticles. The particle form in the photos resembles a sphere and is consistent with previously created ALG/CS nanoparticles. The distribution of particle sizes and the zeta potential are two crucial factors in drug delivery. By using DLS and SEM, the particle size of NPs was verified. The physical characterization of the NPs, including size, zeta potential, PDI, and drug encapsulation effectiveness, is outlined in Table 3. According to the DLS study, the mean hydrodynamic diameter of the *E. angustifolia* -loaded and blank ALG/CS, respectively, is 335.3 nm and 245.1 nm, as shown in Table 3. The PDI value of *E. angustifolia*-loaded ALG/CS NPs was 0.681 as opposed to 0.697 for blank ALG/CS NPs, demonstrating a narrow and desirable particle size distribution. Zeta potential is significant for colloids and suspended nanoparticles. Its worth is directly connected to particle surface shape and suspension stability. The optimized *E. angustifolia* loaded ALG/CS NPs were discovered to have a zeta potential of + 45.1 ± 1 mV.

Table 3
general traits and encapsulation effectiveness of NPs. Data are presented as mean ± SD.

Samples	The polydispersity index (PDI)	Surface charge (mv)	Hydrodynamic diameter (nm)	EE (%)
Free ALG/CS	0.697 ± 0.013	+ 33.0 ± 1	245.1 ± 1.57	---
E. angustifolia + ALG + CS	0.681 ± 0.03	+ 45.1 ± 1	335.3 ± 1.43	83.45 ± 1.97

3.3. E. angustifolia -loaded chitosan NPs: loading efficiency and release kinetics

At various pH levels (3, 5, 7.4) and for more than 72 hours, the *E. angustifolia* extract release pattern from the ALG/CS NPs were examined. When compared to the free *E. angustifolia*, the ALG/CS nanoparticles significantly reduced the initial burst release, with the former releasing around 40–70% of the loaded medication after 24 h and the latter 90% after 8 h (Fig. 2A). After 24 hours, pH 7 enabled an additional 75% release, which continued for 48 hours, but pH 3 and pH 5 did not cause a further firing and stayed at 48% (Fig. 2A). At pH levels of 7.4, 5, and 3, respectively, the entire 72-hour drug release for the improved formulation was 90%, 55%, and 60%. It was determined that the EE of the improved *E. angustifolia* + ALG + CS was 83.45%. The enhancement in the creation of a compact structure of the nanoparticle matrix brought about by the chitosan layer coated on the surface of alginate nanoparticles is what produced an increase in the EE with an increase in the chitosan/alginate mass ratio.

3.4. Detection of MDR bacteria

55 out of the 100 samples that were isolated had methicillin-resistant *S. aureus*, according to microbiological diagnostic tests. Based on the number of samples collected from the hospitals under study, *S. aureus* infection was most prevalent in Shohadaye Tajrish Hospital, where there were 22 patients (or 40 percent), Sasan Hospital had 18 patients (or 32.72percent), and Nikan Hospital had the lowest frequency, with 15 patients (or 27.27 percent) (Table 4). After that, the antibiotic sensitivity of *S. aureus* isolates from different origins was examined, and it was discovered that 44 (80 percent) of the 55 samples tested were MDR. According to the results of the vancomycin screen agar, 30 isolates (68.18%) of the 44 MDR isolates were VDR. In addition, 44 samples of the 44 MDR isolates were capable of creating biofilms. The highest incidence of biofilm production was seen in Shohadaye Tajrish, Sasan, and Nikan hospitals, with 19 (86.36 percent), 15 (83.33 percent), and 10 (66.66 percent) isolates, respectively.

Table 4
Examining the prevalence of *S. aureus* strains derived from various sources that are resistant to methicillin and a number of medications

Total samples	Frequency of MRSA	Frequency of MDR	Resistance Phenotype		Number of VA Resistance Isolates	Biofilm Production			Biofilm Genes		
					VanB Resistance Gene	Total	Biofilm Phenotype	Number	icaA	icaD	pgaB
100	Shohadaye Tajrish Hospital = 22 (40%)	19 (86.36%)	VA, CIP, CD, IPM	8	12	19	Strong	10	+	+	+
			CS, CD, AK	5			moderate	5	+	+	+
			AK, CIP, CD, C	6			Weak	3	+	-	-
							No connection	1	—	—	—
	Nikan = 15 (27.27%)	10 (66.66%)	VA, CD, E, TE, IPM	3	8	10	Strong	7	+	+	+
			C, CIP, CD, TE	5			moderate	2	+	-	+
			VA, CS, IPM, KAN	2			Weak	1	+	-	-
							No connection	0	—	—	—
	Sasan = 18 (32.72%)	15 (83.33%)	VA, CIP, CD, AK	6	10	15	Strong	10	+	+	+
			VA, CAZ, CIP, KAN	5			moderate	3	-	+	+
			VA, CIP, CD, CS, TE	4			Weak	2	—	—	—
							No connection	0	—	—	—
Total	55 (55%)	44 (80%)	44 (80%)		30 (68.18%)	44	Strong Sum = 9		Moderate Sum= 3.33		Weak Sum = 2

AK: Amikacin, E: Erythromycin, C: Chloramphenicol, CIP: Ciprofloxacin, IPM: Imipenem, CS: colistin, TE: tetracycline, CD: clindamycin, VA: vancomycin, CAZ: ceftazidime, MDR: multidrug-resistant, MRSA: methicillin-resistant *Staphylococcus aureus*.

3.5. Biofilm formation

The MRSA phenotype was present in 55 (55%) of the isolates, while MDR was present in 44 (80%). 30 (68.18%) of the isolates that were analyzed had vancomycin resistance (Table 4). In order to test for antibiotic sensitivity, Table 4 contains the findings. Collected isolates that showed resistance to at least three or more antibiotic classes were considered MDR. All MDR strains

exhibited biofilm development, and there was a connection between MDR and biofilm formation. The four isolates from Samples 8, 12, 13, and 22 were chosen as the bacteria that produced biofilms, together with the control sample of *S. aureus* ATCC 33592. The ability of collected isolates from sources to produce biofilms on polystyrene microtiter plates in a TSB medium demonstrated robust biofilm formation (Fig. 3).

3.6. Antimicrobial activity

3.6.1. Minimum inhibitory concentration and minimum bactericidal concentration

Table 5 displays the MIC and MBC values of free *E. angustifolia*, *E. angustifolia*-loaded NPs, and empty NPs against *S. aureus* ATCC 33592 and isolated MRSA strains. Results showed that in contrast to the free extract, which had no bactericidal action, the ALG/CS-encapsulated extract's MIC was discovered to be 4 to 32 times lower (Table 4). The values of MBC in some strains were similar to MIC, while in other strains, the MBC values were higher. Table 5 shows that the combination of chitosan and alginate nanoparticles alone does not have an inhibitory and bactericidal effect against isolated methicillin-resistant strains. As a result, empty NPs had no antimicrobial action. Notably, none of the 4 *S. aureus* strains tested were susceptible to the free *E. angustifolia*'s intrinsic bactericidal effects.

Table 5. MIC and MBC values of selected MRSA samples and *E. angustifolia* extract encapsulated in ALG/CS.

Microorganism	Free *E. angustifolia*		ALG/CS		*E. angustifolia*- ALG/CS NPs	
	MIC (µg/ml)	MBC (µg/ml)	MIC (µg/ml)	MBC (µg/ml)	MIC (µg/ml)	MBC (µg/ml)
Sample 8	128	256	64	128	8	16
Sample 12	64	128	128	256	4	4
Sample 13	128	256	32	64	4	8
Sample 22	64	128	64	128	2	4
ATCC 33592	32	64	32	64	1	2

3.6.2. Well Diffusion

Figure 4E. *angustifolia*-ALG/CS NPs in the current investigation demonstrated significant antibacterial efficacy against MDR *S. aureus* (samples 8, 12, 13, and 22). Observing the clear area around the wells indicates the inhibition of bacterial growth by the synthesized nanoparticles (Fig. 4). Our results showed that nanoparticles synthesized with *E. angustifolia* extract could inhibit the growth of all 4 strains of multi-drug resistant *S. aureus* in sub-MIC concentration. As a consequence, Fig. 4 displays a good diffusion test that confirms *E. angustifolia*-ALG/CS NPs were superior to free extract and free ALG/CS NPs as antibacterial agents on *S. aureus*.

3.6.3. NPs anti-Biofilm activity

The effectiveness of the synthesized ALG/CS NPs encapsulated with *E. angustifolia* against the biofilm development of isolated MDR samples was evaluated since biofilm, which accounts for 65–80% of all infections, is a common source of antibiotic resistance. As shown in Fig. 5, biofilm suppression was seen with sub-MIC concentrations of *E. angustifolia*-loaded NPs, demonstrating the significant magnitude of biofilm inhibition. Comparing *E. angustifolia* ALG/CS NPs to free *E. angustifolia*, it was found that the biofilm production was significantly reduced (*** $p < 0.001$) (Fig. 5). In comparison to *E. angustifolia*-loaded NPs at the same range of therapeutic concentration, free NPs showed slightly reduced biofilm formation. Due to this, *E. angustifolia* ALG/CS NPs are efficient antibacterial drug carriers for the removal of biofilm. In this investigation, encapsulation allowed for more efficient biofilm clearing with a 1 to 10 fold reduced sub-MIC of free *E. angustifolia*.

3.6.4. Assessment of biofilm gene expression

In order to confirm the inhibitory effect of NPs synthesized with *E. angustifolia* extract on biofilm formation, the expression of genes related to biofilm (*IcaD*, *IcaA*, and *IcaC*) was evaluated using a real-time PCR technique. The change in gene expression was evaluated before and after treatment of isolated strains with free NPs, free *E. angustifolia*, and *E. angustifolia*-encapsulated

ALG/CS at a concentration of sub-MIC. The results demonstrated that *E. angustifolia*-encapsulated ALG/CS significantly inhibited the expression of the *IcaD*, *IcaA*, and, *IcaC* genes in all MDR strains (***$p < 0.0001$) (Fig. 6). In addition, the expression of these genes in the isolated strains that were treated with free extract and free NPs had not a significant decrease compared to the encapsulated extract.

3.7. MTT assay

The cytotoxicity of free extract, free NPs, and *E. angustifolia*-encapsulated ALG/CS at varying doses, 1 to 256 µM/ml on HEK 293 cell lines over 24 h, was assessed using the MTT test. *E. angustifolia*-encapsulated ALG/CS did not exhibit any possible cytotoxicity compared to the control group (the cells that had only been exposed to medium) at doses of 1to 250 µM/ml for 24 h. Also, the results showed that the free extract at a dose of 250 µM/ml had the highest cytotoxicity on HEK 293 cell line (survival rate less than 70%) (Fig. 7). The delayed release of *E. angustifolia* from the ALG/CS compared to the free form may cause the extract's lowered toxicity. Compared to the free form, only about half of the *E. angustifolia* is released from NPs after a 24-hour contact. Cell viability for the free extract, free NPs, and *E. angustifolia*-NPs at 256 M was 57.5%, 85.5%, and 90.5%, respectively (Fig. 7).

4. Discussion

The emergence of the MRSA epidemic has encouraged new antibacterial agent research and the development of creative strategies (Rasmussen et al., 2011). Plant-based antimicrobial agents have become more significant in treating infectious ailments in recent years due to the rise of antibiotic-resistant pathogens (Celebi et al., 2021). Antibacterial activity in formulations has drawn increased scientific attention as one of the possible uses of chitosan-alginate-based nanomaterials. Therefore, this study investigated the antibacterial and anti-biofilm effects of *E. angustifolia* extract encapsulated in chitosan and alginate NPs.

By using ionotropic gelation and a previously known ratio of 1:0.5:0.5 between *E. angustifolia*, CS, and ALG, the nanoparticles were loaded with *E. angustifolia*. In this ratio, the encapsulation efficiency was reported as 83.45%. According to the DLS examination, the synthetic *E. angustifolia* NPs had a high mono-dispersity and a spherical form (Fig. 2). The optimal *E. angustifolia* concentration for loading nanoparticles was determined to be 1g/ml. The final *E. angustifolia*-loaded alginate-chitosan nanoparticle formulation had a mean diameter of 335.3 nm and a PDI of 0.681. Since DLS evaluates the hydrodynamic diameter, the sizes acquired using the DLS approach were bigger than those obtained using SEM. The physical condition of the nanoparticles at the time of measurement is the cause of this variance (Nagarwal et al., 2012). When analyzed using DLS, gel nanoparticles such as calcium-alginate and chitosan are in a swollen state in water (seven times the size of their dried counterparts) but collapse once the sample is dried out before being viewed using TEM or SEM, eliminating the swelling effect. Similar to this, earlier research on alginate-chitosan nanoparticles showed 4–5 times lower particle sizes than those seen with DLS (Sarmento et al., 2007; Katuwavila et al., 2016). As is typical of polymeric particles, the PDI of the blank and loaded CS/ALG NPs was lower. The PDI is a number that varies from 0 to 1. The better the particle size uniformity, the closer this value is to zero.

The CS/ALG and *E. angustifolia* CS/ALG NPs had high positive values in their zeta potentials, indicating the stability of the colloidal suspensions (Table 3). When employing NPs for medication administration, positively charged surfaces are a bonus since they allow them to go through cell membrane negative channels more efficiently (Bhunchu et al., 2015). This information indicates that this formulation is reliable. By using FTIR, it was proven that *E. angustifolia* was successfully encapsulated within the alginate nanoparticles. Figure 1 displays the spectra of empty NPs, *E. angustifolia*-loaded CS/ALG nanoparticles, and pure *E. angustifolia*. The hydrogen bonding between the carboxyl and amino groups of alginate and chitosan is responsible for the alterations in the FT-IR spectra created by the carboxyl groups, amino groups, and amide bonds, indicating the production of CS/ALG NPs. The loading of *E. angustifolia* without causing any changes to its chemical structure was confirmed by absorption peaks at 1088, 1639, 2426, and 3435 cm^{-1} in loaded nanoparticles comparable to *E. angustifolia*. The results are consistent with information from earlier publications (Bhunchu et al., 2015; Moghtaderi et al., 2021; Chavanpatil et al., 2007). The targeted medicine benefits greatly from nanocarriers. However, these systems are useless if the drug is not released effectively from the encapsulation (Rizvi et al., 2018). Compared to pH 3 and 5, pH 7.4 causes the bioactive *E. angustifolia* to extract to remove more quickly (Lim et al., 2017). The overall structure of chitosan and alginate is affected by pH in a way that is related to the state of the ionization of amino and carboxylate groups (Lim et al., 2017). The amount of H + in an acidic solution (pH 3, 5) is high. Ion H

+ penetrates the network microcapsules and balances the electrostatic force of attraction (Nalini et al., 2019). It results in a low relaxation rate, which slows the *E. angustifolia* extract's release rate. At pH ≥ 7, amine groups are deprotonated and begin to reject the negatively charged carboxylate group, weakening the connection between the two groups (Lim et al., 2017). As a consequence, CS/ALG nanoparticles release bioactive substances more quickly. The work supports findings that quercetin is released more rapidly from CS/ALG NPs at pH 7.4 than at pH 5.5 or 6.5 (Yousefi et al., 2020). According to other research, viola-odorata encapsulation in alginate chitosan beads suggested low release at pH 1.5 and increased release at pH 7 (Chen et al., 2019).

Due to the rising occurrence of isolates that are multidrug resistant, treatment options for infections caused by microbial resistant organisms are becoming more constrained (Choo et al., 2016). The results of this study showed that 55% of isolates isolated from different sources of infection were resistant to methicillin. Also, 80% of isolates were resistant to several antibiotics (Table 4). Despite the fact that vancomycin is the antibiotic of choice for MRSA treatment (Sharma et al., 2019), the issue is exacerbated worse by the high frequency of vancomycin resistance (68.18%). The most of the isolated organisms also produced biofilms, further aggravating the treatment problem. Clinicians' ability to provide effective antibiotic treatment has been severely hampered by the rise of MDR isolates in human infections (Nourbakhsh et al., 2016). The literature has reported a number of resistance-determinants (both inherent resistance and genes acquired on mobile genetic components), which enable bacteria to endure antibiotic dosages that would otherwise be deadly (Nourbakhsh et al., 2016). In addition to these resistance-determinants, bacterial biofilm development is a significant contributor to treatment failures. In a protective extracellular matrix, bacterial colonies of one or more species form biofilms. Exopolysaccharides (EPS), environmental DNA (eDNA), proteins, surfactants, lipids, and water make up the majority of this matrix (Nourbakhsh et al., 2016). On inanimate objects and within the body, biofilms enable bacterial colonies to adhere to and endure (Nourbakhsh et al., 2016). In these conditions, it has become crucial to develop a substitute method that, while having minimal toxicity, has effective antibacterial and anti-biofilm effects on the relevant strain. In this study, chitosan and alginate natural polymers were used as nano-carrier. Compared to other nanoparticles, these natural nanoparticles are thought to be less harmful and biosafe (Bhunchu et al., 2015). The lower MIC value confirmed the antibacterial activity of synthzied NPs when compared to free extract (Table 5). *E. angustifolia* NPs were shown to impede MRSA's ability to build both early and mature biofilms. Also, our results confirmed that the extract encapsulated with chitosan and alginate significantly inhibits biofilm formation in multi-drug resistant *S. aureus* strains. Additionally, the impact of *E. angustifolia* nanoparticles at half their maximum inhibitory concentration (MIC) on the expression of the *IcaD*, *IcaA*, and *IcaC* genes was examined. Polysaccharide intracellular adhesion (PIA), which is expressed by the ica operon (*icaABCD*), modulates interactions between *S. aureus* and abiotic hydrophilic surfaces (Ahmed et al., 2019). Since the *icaA* and *icaD* genes are thought to be essential for intercellular adhesion, it is reasonable to conclude that these genes are solely significant for the creation of the bacterial multilayer during the generation of biofilms (Liu et al., 2020). In the present work, *E. angustifolia* NPs dramatically reduced the expression of the *icaA*, *icaD* and, *icaC* genes. However, gene expression was not reduced in the groups treated with empty extract and empty nanoparticles. These results show that nanoparticles made with their unique mechanism can prevent the initial attachment of bacteria and biofilm formation.

The agar well diffusion experiment findings demonstrated the *E. angustifolia* NPs' significant efficacy against all four MDR bacteria. When compared to the free form of *E. angustifolia* and NPs, all of the tested strains had a broader zone of inhibition against the *E. angustifolia* ALG/CS NPs, indicating that the strains were more sensitive to the NPs. The presence of long aliphatic chains in the nanoparticle structure may be the reason for the strains' sensitivity (Wang et al., 2019; Thaya et., 2018). The ionic charges on the formulation's surface may have reacted with the charges on the bacterial cell wall's constituents to disturb the wall's structure (Wang et al., 2019). In line with the results obtained from this research, Rajagopalan Thaya et al. showed that nanoparticles synthesized from chitosan and alginate have the ability to inhibit the growth of multi-drug-resistant bacteria (Thaya et., 2018). The findings imply that because chitosan has a positive charge, it may readily interact with negatively charged bacterial cell membranes to prevent bacterial development. The fusing of CS/ALG with the bacterial cell membrane, which resulted in its direct connection with the cell membrane and enabled the extract to discharge to the environment, may account for the more potent antibacterial activity of the encapsulated CS/ALG than that of the free extract. It has been noted that fusing the CS/ALG structure with the bacterial outer membrane increases the antibacterial properties. Additionally, *E. angustifolia*-loaded niosomes showed substantial antibacterial efficacy against *Klebsiella pneumoniae*, according to Moghtaderi

et al (Moghtaderi et al., 2021). In addition, the toxicity of free extract, nanoparticles and encapsulated nanoparticles on HEK 93 cell line was evaluated. Free CS/ALG at a concentration of 256 µM is not toxic, which makes it an attractive material for nanocarriers. Additionally, the slower release of *E. angustifolia* from CS/ALG might account for the encapsulated extract's decreased toxicity compared to the free *E. angustifolia* (Barani et al., 2019).

5. Conclusion

In conclusion, to successfully deliver bioactive plant extracts, chitosan-alginate core-shell nanoparticles with E. angustifolia loaded on them were created. SEM, DLS, and FT-IR spectroscopy were used to characterize the synthesized *E. angustifolia* CS/ALG NPs. Using the MTT test, the cytotoxicity of the chitosan-alginate nanoparticles was also assessed. The chitosan-alginate nanoparticles only exhibit minimal toxicity at extremely high concentrations, according to the MTT experiment. The results of the antimicrobial activity test show that nanoparticles encapsulated with *E. angustifolia* extracts can perform better than some commercial antibiotics against resistant *S. aureus.* Also, in this study, we showed that the manufactured nanoparticles significantly reduce the expression of essential genes in biofilm formation. Finally, this study aimed to help treat multi-drug resistant infectious diseases using nanoparticles and natural compounds. Additional research is required to determine the plant extracts' active ingredients and to understand the underlying process. The findings of this study provide a fantastic chance to use natural polymers to boost the antibacterial activity of plant extracts.

Declarations

Acknowledgments

The AmitisGen Med Tech Group provided the required laboratory resources for this investigation, and the authors would like to thank them for their assistance.

Consent for publication

Not applicable.

Availability of data and materials

All data analyzed during this study are included in this published article.

Competing interests

The authors declare that they have no competing interests.

Funding

No particular grant was given to this research by funding organizations in the public, private, or not-for-profit sectors.

Authors’ contributions

ST and ZZ carried out the sampling and culture method. SK-S and HK participated in the design of the study, performed the statistical analysis and writing the manuscript. NR carried out the molecular genetic studies, participated in the primers sequence. TP-G is responsible for doing the whole project and submitting the article.

References

1. Assis LM, Nedeljković M, Dessen A (2017) New strategies for targeting and treatment of multi-drug resistant Staphylococcus aureus. Drug Resistance Updates, 31,1–14
2. Ahmed DM, Messih MAWA, Ibrahim NH, Meabed MH, Abdel-Salam SM (2019) Frequency of icaA and icaD determinants and biofilm formation among coagulase-negative staphylococci associated with nasal carriage in neonatal intensive care units.

Germs, 9(2),61

3. Bajaj T, Karapetians A, Karapetians N, Duong H, Heidari A (2020) Methicillin resistant Staphylococcus aureus infective endocarditis presenting as neutrophilic meningoencephalitis. AME Case Reports, 4
4. Banerjee S, Vishakha K, Das S, Dutta M, Mukherjee D, Mondal J, Ganguli A (2020) Antibacterial, anti-biofilm activity and mechanism of action of pancreatin doped zinc oxide nanoparticles against methicillin resistant Staphylococcus aureus. Colloids and surfaces B: Biointerfaces, 190,110921
5. Barani M, Mirzaei M, Torkzadeh-Mahani M, Adeli-Sardou M (2019) Evaluation of carum-loaded niosomes on breast cancer cells: Physicochemical properties, in vitro cytotoxicity, flow cytometric, DNA fragmentation and cell migration assay. Scientific reports, 9(1),1–10
6. Banoub NG, Saleh SE, Helal HS, Aboshanab KM (2021) Antibiotics Combinations and Chitosan Nanoparticles for Combating Multidrug Resistance Acinetobacter baumannii. Infection and Drug Resistance, 14,3327
7. Bhunchu S, Rojsitthisak P (2014) Biopolymeric alginate-chitosan nanoparticles as drug delivery carriers for cancer therapy. Die Pharmazie-An International Journal of Pharmaceutical Sciences, 69(8),563–570
8. Bhunchu S, Rojsitthisak P, Rojsitthisak P (2015) Effects of preparation parameters on the characteristics of chitosan–alginate nanoparticles containing curcumin diethyl disuccinate. Journal of Drug Delivery Science and Technology, 28,64–72
9. Celebi D, Cinisli KT, Celebi O (2021) NanoBio challenge: Investigation of antimicrobial effect by combining ZnO nanoparticles with plant extract Eleagnus angustifolia. Materials Today: Proceedings, 45, 3814–3818
10. Chen X, Lou W, Liu J, Ding B, Fan W, Hong J (2019) A novel antimicrobial polymer efficiently treats multidrug-resistant MRSA-induced bloodstream infection. Bioscience Reports, 39(10)
11. Choo EJ, Chambers HF (2016) Treatment of methicillin-resistant Staphylococcus aureus bacteremia. Infection & chemotherapy, 48(4),267–273
12. Dey R, De K, Mukherjee R, Ghosh S, Haldar J (2019) Small antibacterial molecules highly active against drug-resistant Staphylococcus aureus. MedChemComm, 10(11),1907–1915
13. Di Martino A, Trusova ME, Postnikov PS, Sedlarik V (2018) Folic acid-chitosan-alginate nanocomplexes for multiple delivery of chemotherapeutic agents. J Drug Deliv Sci Technol 47:67–76
14. El-Far A, Samir S, El-Gebaly E, Taha NY, Fahmy EM, Diab TM, El-Shenawy A (2021) Assessment of eugenol inhibitory effect on biofilm formation and biofilm gene expression in methicillin resistant Staphylococcus aureus clinical isolates in Egypt. Infection, Genetics and Evolution, 89,104722
15. Ghajari G, Nabiuni M, Amini E (2021) The association between testicular toxicity induced by Li2Co3 and protective effect of Ganoderma lucidum: Alteration of Bax & c-Kit genes expression. Tissue and Cell, 72,101552
16. Gombotz WR, Wee S (1998) Protein release from alginate matrices. Advanced drug delivery reviews, 31(3),267–285
17. Jacob J, Haponiuk JT, Thomas S, Gopi S (2018) Biopolymer based nanomaterials in drug delivery systems: A review. Materials today chemistry, 9,43–55
18. Kaur J, Kour A, Panda JJ, Harjai K, Chhibber S (2020) Exploring endolysin-loaded alginate-chitosan nanoparticles as future remedy for Staphylococcal Infections. AAPS PharmSciTech, 21(6),1–15
19. Katuwavila NP, Perera ADL, Samarakoon SR, Soysa P, Karunaratne V, Amaratunga GA, Karunaratne D (2016) Chitosan-alginate nanoparticle system efficiently delivers doxorubicin to MCF-7 cells. Journal of Nanomaterials, 2016
20. Kumar P (2020) A review on quinoline derivatives as anti-methicillin resistant Staphylococcus aureus (MRSA) agents. BMC chemistry, 14(1),1–14
21. Lertsutthiwong P, Rojsitthisak P, Nimmannit U (2009) Preparation of turmeric oil-loaded chitosan-alginate biopolymeric nanocapsules. Materials Science and Engineering: C, 29(3),856–860
22. Li P, Dai YN, Zhang JP, Wang AQ, Wei Q (2008) Chitosan-alginate nanoparticles as a novel drug delivery system for nifedipine. International journal of biomedical science: IJBS, 4(3),221
23. Lim GP, Ahmad MS (2017) Development of Ca-alginate-chitosan microcapsules for encapsulation and controlled release of imidacloprid to control dengue outbreaks. Journal of industrial and engineering chemistry, 56,382–393

24. Liu H, Hu Y, Zhu Y, Wu X, Zhou X, Pan H, Tian P (2020) A simultaneous grafting/vinyl polymerization process generates a polycationic surface for enhanced antibacterial activity of bacterial cellulose. International journal of biological macromolecules, 143,224–234
25. Mahmoudi H, Pourhajibagher M, Chiniforush N, Soltanian AR, Alikhani MY, Bahador A (2019) Biofilm formation and antibiotic resistance in meticillin-resistant and meticillin-sensitive Staphylococcus aureus isolated from burns. Journal of wound care, 28(2),66–73
26. Mariana NS, Salman SA, Neela V, Zamberi S (2009) Evaluation of modified Congo red agar for detection of biofilm produced by clinical isolates of methicillin resistance Staphylococcus aureus. African Journal of Microbiology Research, 3(6),330–338
27. Mistrikova I, Vaverkova S (2006) Echinacea—chemical composition, immunostimulatory activities and uses. Thaiszia J Bot, 16,11–26
28. Mirzaie A, Peirovi N, Akbarzadeh I, Moghtaderi M, Heidari F, Yeganeh FE, Bakhtiari R (2020) Preparation and optimization of ciprofloxacin encapsulated niosomes: A new approach for enhanced antibacterial activity, biofilm inhibition and reduced antibiotic resistance in ciprofloxacin-resistant methicillin-resistance Staphylococcus aureus. Bioorganic Chemistry, 103,104231
29. Moghtaderi M, Mirzaie A, Zabet N, Moammeri A, Mansoori-Kermani A, Akbarzadeh I, Ren Q (2021) Enhanced antibacterial activity of Echinacea angustifolia extract against multidrug-resistant Klebsiella pneumoniae through niosome encapsulation. Nanomaterials, 11(6),1573
30. Nagarwal RC, Kumar R, Pandit JK (2012) Chitosan coated sodium alginate–chitosan nanoparticles loaded with 5-FU for ocular delivery: In vitro characterization and in vivo study in rabbit eye. European Journal of Pharmaceutical Sciences, 47(4),678–685
31. Nalini T, Basha SK, Sadiq AMM, Kumari VS, Kaviyarasu K (2019) Development and characterization of alginate/chitosan nanoparticulate system for hydrophobic drug encapsulation. Journal of Drug Delivery Science and Technology, 52,65–72
32. Nourbakhsh F, Namvar AE (2016) Detection of genes involved in biofilm formation in Staphylococcus aureus isolates. GMS Hygiene and infection control, 11
33. Pan Y, Li YJ, Zhao HY, Zheng JM, Xu H, Wei G, Hao JS (2002) Bioadhesive polysaccharide in protein delivery system: chitosan nanoparticles improve the intestinal absorption of insulin in vivo. International journal of pharmaceutics, 249(1–2),139–147
34. Piri-Gharaghie T, Beiranvand S, Riahi A, Shirin NJ, Badmasti F, Mirzaie A, Hajrasouliha S (2022) Fabrication and characterization of thymol-loaded chitosan nanogels: Improved antibacterial and anti-biofilm activities with negligible cytotoxicity. Chemistry & Biodiversity, 19(3), e202100426
35. Prasetyaningrum A, Arrois S, Lafifa F, Mubarok AZ, Fani F, Handayani NA, Jos B Encapsulation of Lemongrass Extract (Cymbopogon citratus) Coated Alginate/Chitosan Using Gelation Method. Reaktor, 21(3),124–132
36. Rasmussen RV, Fowler VG Jr, Skov R, Bruun NE (2011) Future challenges and treatment of Staphylococcus aureus bacteremia with emphasis on MRSA. Future microbiology, 6(1),43–56
37. Rinaldi F, Del Favero E, Moeller J, Hanieh PN, Passeri D, Rossi M, Fratoddi I (2019) Hydrophilic silver nanoparticles loaded into niosomes: Physical–chemical characterization in view of biological applications. Nanomaterials, 9(8),1177
38. Rizvi SA, Saleh AM (2018) Applications of nanoparticle systems in drug delivery technology. Saudi pharmaceutical journal, 26(1),64–70
39. Roca I, Akova M, Baquero F, Carlet J, Cavaleri M, Coenen S, Vila J (2015) The global threat of antimicrobial resistance: science for intervention. New microbes and new infections, 6,22–29
40. Sarmento B, Ribeiro A, Veiga F, Sampaio P, Neufeld R, Ferreira D (2007) Alginate/chitosan nanoparticles are effective for oral insulin delivery. Pharmaceutical research, 24(12),2198–2206
41. Scolari IR, Páez PL, Musri MM, Petiti JP, Torres A, Granero GE (2020) Rifampicin loaded in alginate/chitosan nanoparticles as a promising pulmonary carrier against Staphylococcus aureus. Drug Delivery and Translational Research, 10(5),1403–1417

42. Sharma D, Misba L, Khan AU (2019) Antibiotics versus biofilm: an emerging battleground in microbial communities. Antimicrobial Resistance & Infection Control, 8(1),1–10
43. Shukla A, Singha RK, Sasaki T, Prasad VVDN, Bal R (2019) Preparation of Nanostructured Pd-Fe2O3 Catalyst for C–C Coupling Reaction. ChemistrySelect, 4(35),10566–10575
44. Sharifi-Rad M, Mnayer D, Morais-Braga MFB, Carneiro JNP, Bezerra CF, Coutinho HDM, Sharifi-Rad J (2018) Echinacea plants as antioxidant and antibacterial agents: From traditional medicine to biotechnological applications. Phytotherapy Research, 32(9),1653–1663
45. Smidsrød O, Skja G (1990) Alginate as immobilization matrix for cells. Trends in biotechnology, 8,71–78
46. Sohrabi S, Haeri A, Mahboubi A, Mortazavi A, Dadashzadeh S (2016) Chitosan gel-embedded moxifloxacin niosomes: an efficient antimicrobial hybrid system for burn infection. International journal of biological macromolecules, 85,625–633
47. Targhi AA, Moammeri A, Jamshidifar E, Abbaspour K, Sadeghi S, Lamakani L, Akbarzadeh I (2021) Synergistic effect of curcumin-Cu and curcumin-Ag nanoparticle loaded niosome: Enhanced antibacterial and anti-biofilm activities. Bioorganic Chemistry, 115,105116
48. Tan Y, Ma S, Leonhard M, Moser D, Haselmann GM, Wang J, Schneider-Stickler B (2018) Enhancing antibiofilm activity with functional chitosan nanoparticles targeting biofilm cells and biofilm matrix. Carbohydrate polymers, 200,35–42
49. Thaya R, Vaseeharan B, Sivakamavalli J, Iswarya A, Govindarajan M, Alharbi NS, Benelli G (2018) Synthesis of chitosan-alginate microspheres with high antimicrobial and antibiofilm activity against multi-drug resistant microbial pathogens. Microbial pathogenesis, 114,17–24
50. Wang S, Song J, Li Y, Zhao X, Chen L, Li G, Ge X (2019) Grafting antibacterial polymer brushes from titanium surface via polydopamine chemistry and activators regenerated by electron transfer ATRP. Reactive and Functional Polymers, 140,48–55
51. Yousefi M, Khanniri E, Shadnoush M, Khorshidian N, Mortazavian AM (2020) Development, characterization and in vitro antioxidant activity of chitosan-coated alginate microcapsules entrapping Viola odorata Linn. extract. International Journal of Biological Macromolecules, 163,44–54

Figures

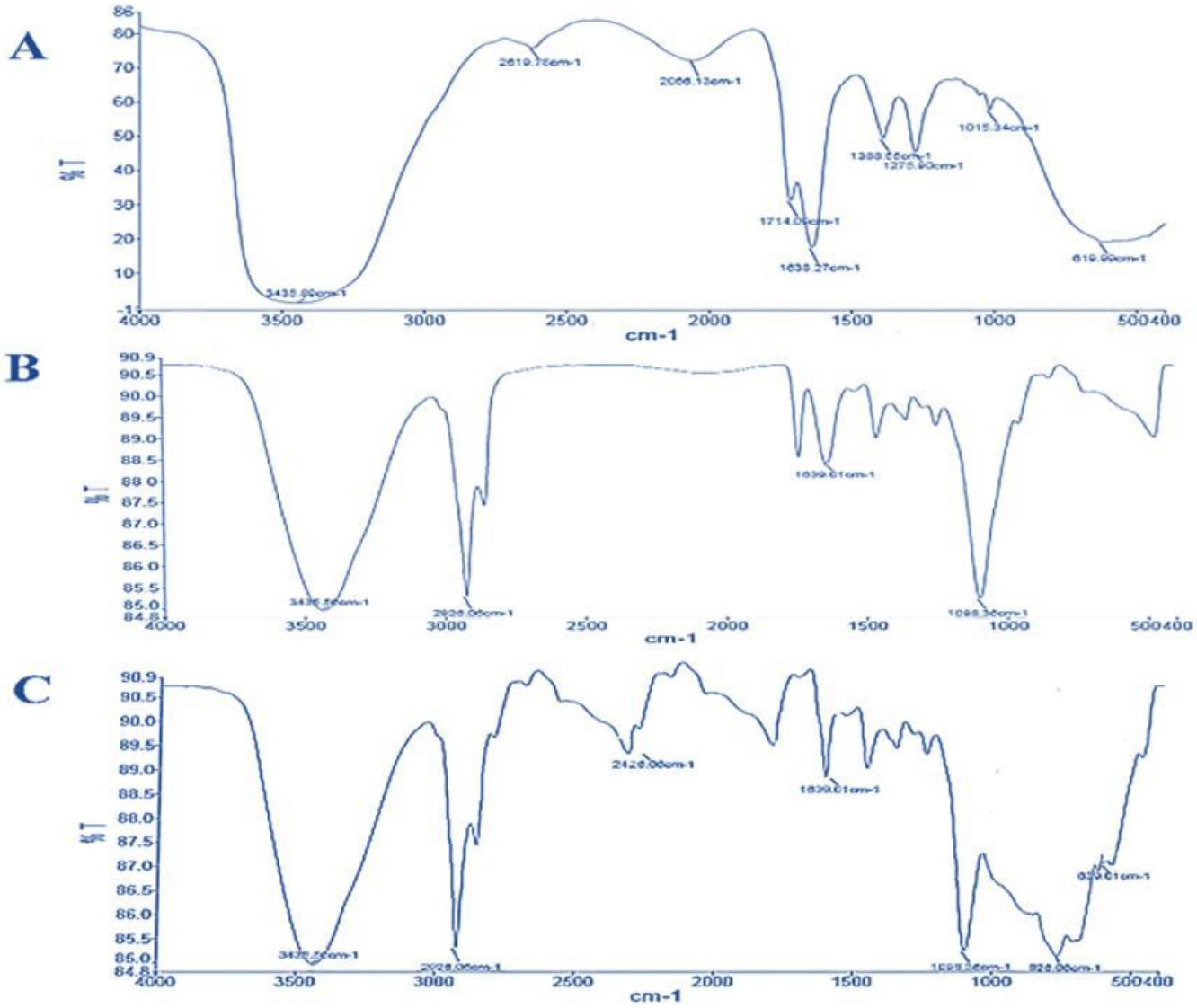

Figure 1

FTIR spectra of blank *E. angustifolia* extract (A), empty (B), and *E. angustifolia* -loaded chitosan-alginate nanoparticles (c).

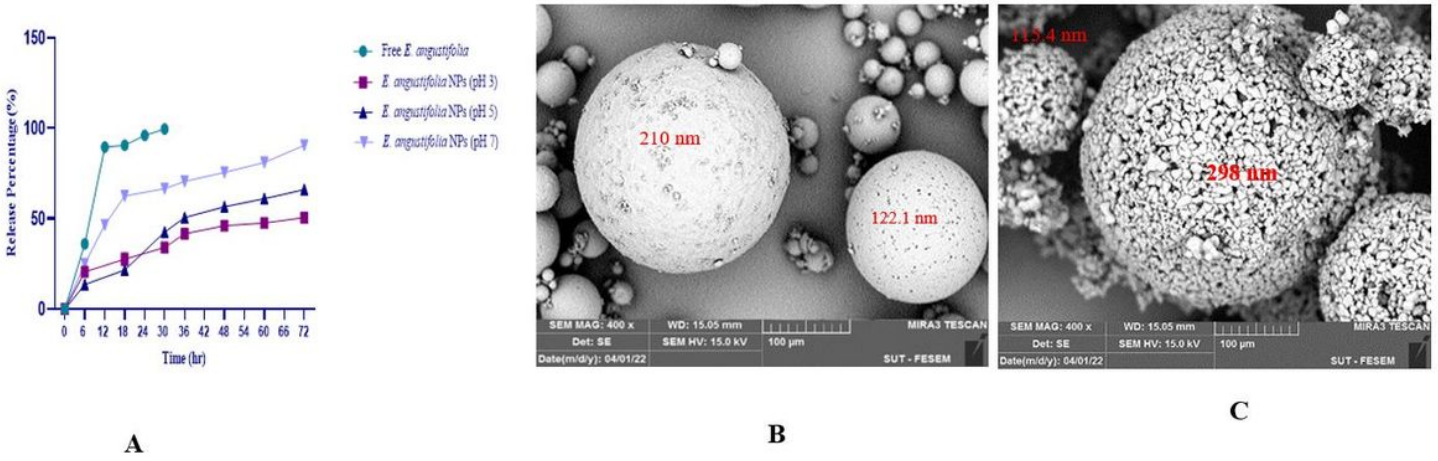

Figure 2

(A) *E. angustifolia*cumulative percentage release over time from *E. angustifolia* ALG/CS NPs and the free *E. angustifolia*, using different pH. SEM analysis of the *E. angustifolia* ALG/CS NPs that were synthesized (B) surface morphology of blank ALG and CS (C) ALG/CS containing *E. angustifolia.*

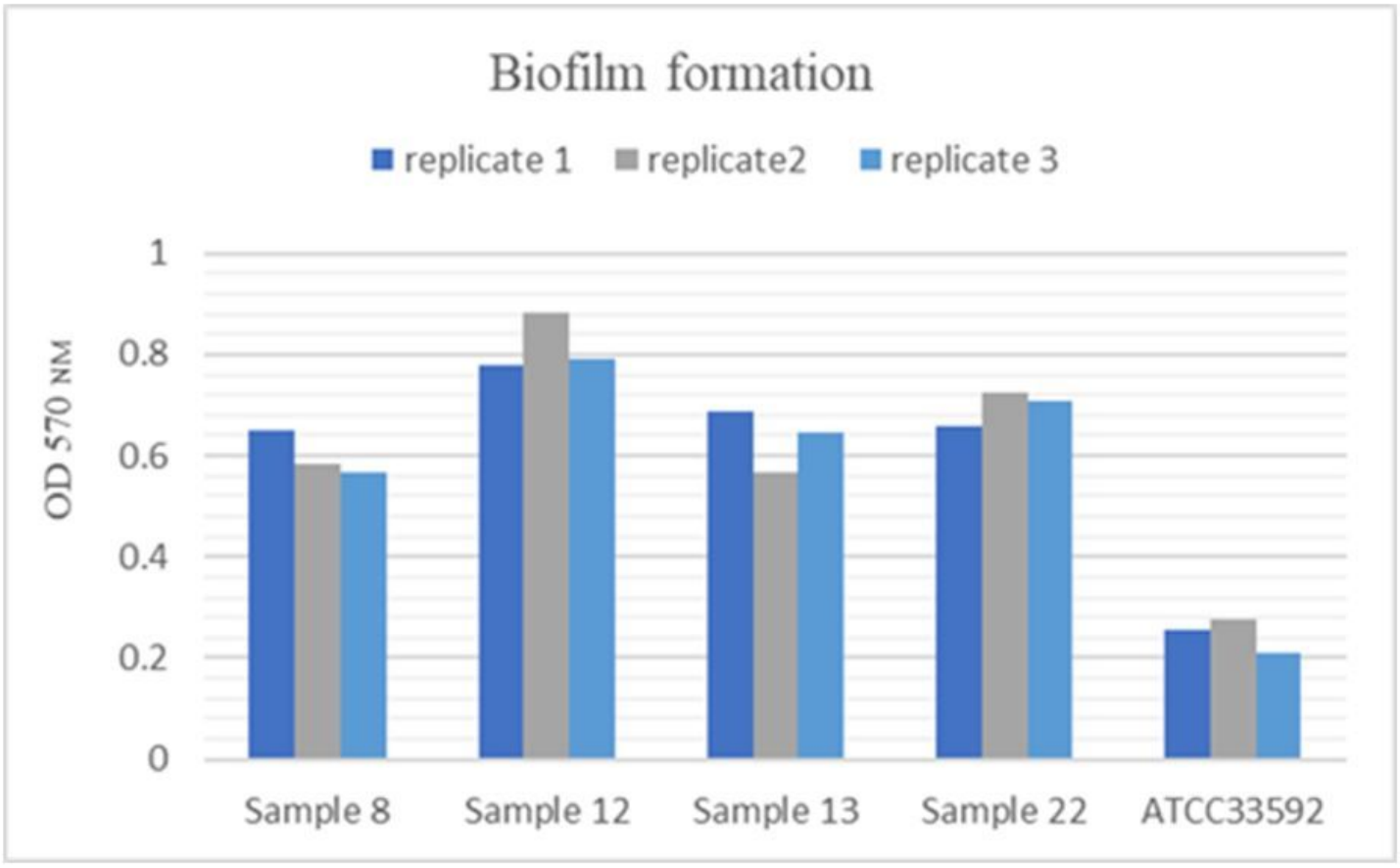

Figure 3

MRSA and MDR strains' isolated micro-pattern biofilm development. The outcomes were calculated as the mean of the OD value and standard deviation (SD) from three separate replicates.

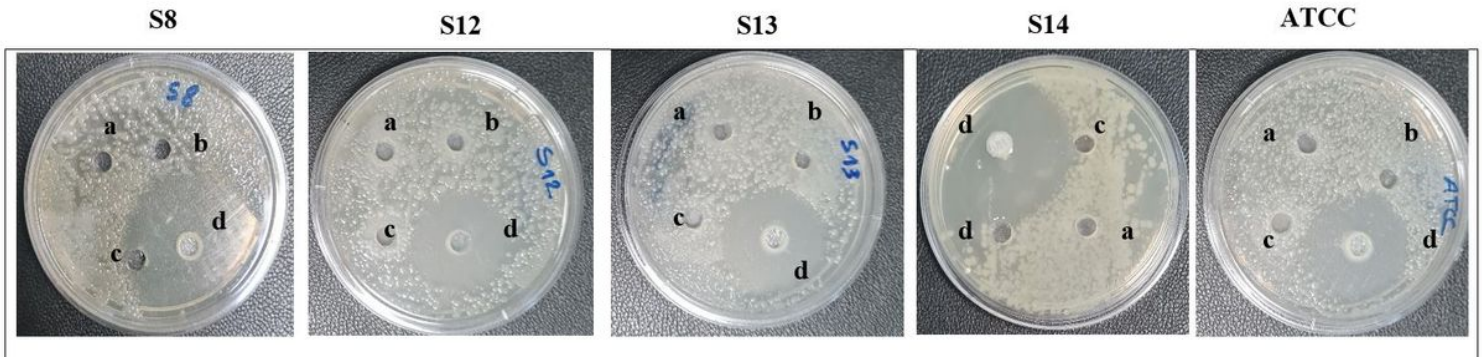

Figure 4

Investigating the impact of *E. angustifolia*-ALG/CS NPs on MDR-resistant isolates of *S. aureus*using a well diffusion experiment. (a) control negative, (b) free NPs, (c) free extract, (d) *E. angustifolia*-ALG/CS NPs.

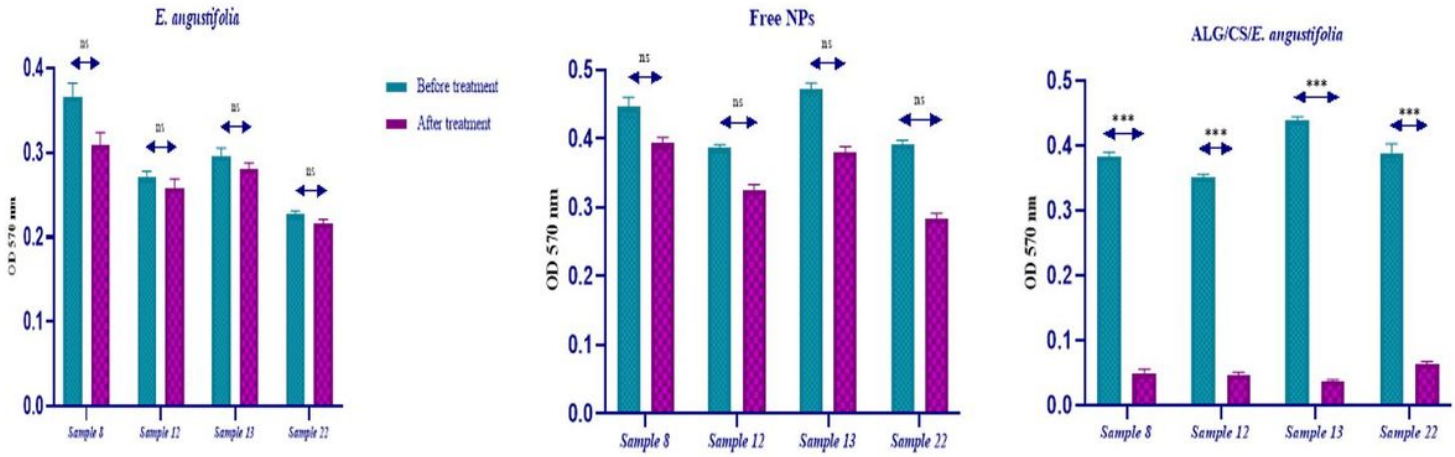

Figure 5

Inhibition of MDR *S. aureus* strains' ability to produce biofilms after various treatments. The data are mean with standard deviation, ***p <0.001, and ns: not significant.

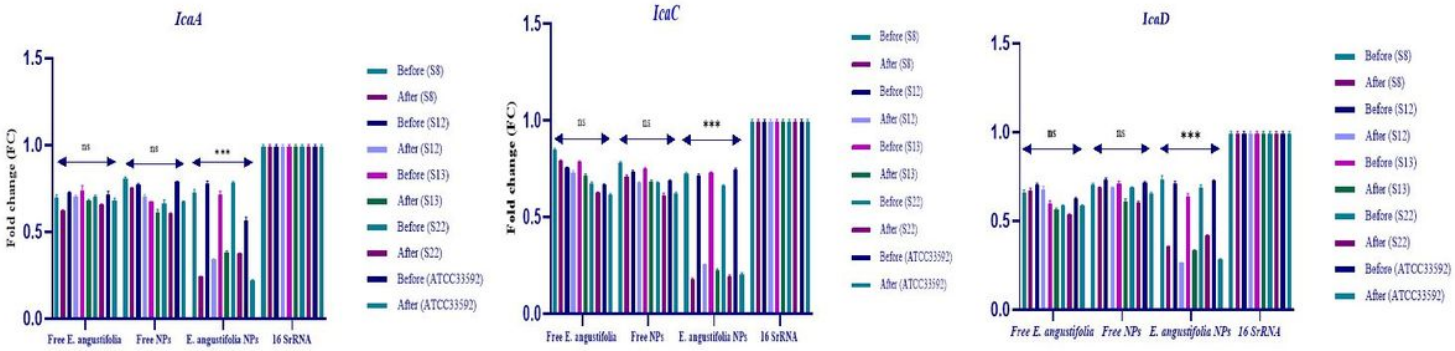

Figure 6

Quantitative real-time PCR analysis was used to assess the relative expression of genes related to biofilm formation in MDR S. aureus. Total RNA from the bacteria in the various treatment groups (free extract, free NPs, and *E. angustifolia*-encapsulated

ALG/CS) was harvested, converted to cDNA, and then subjected to qPCR analysis using specific primers. Data represented as mean ± SD *** p<0.001, ns: not significant.

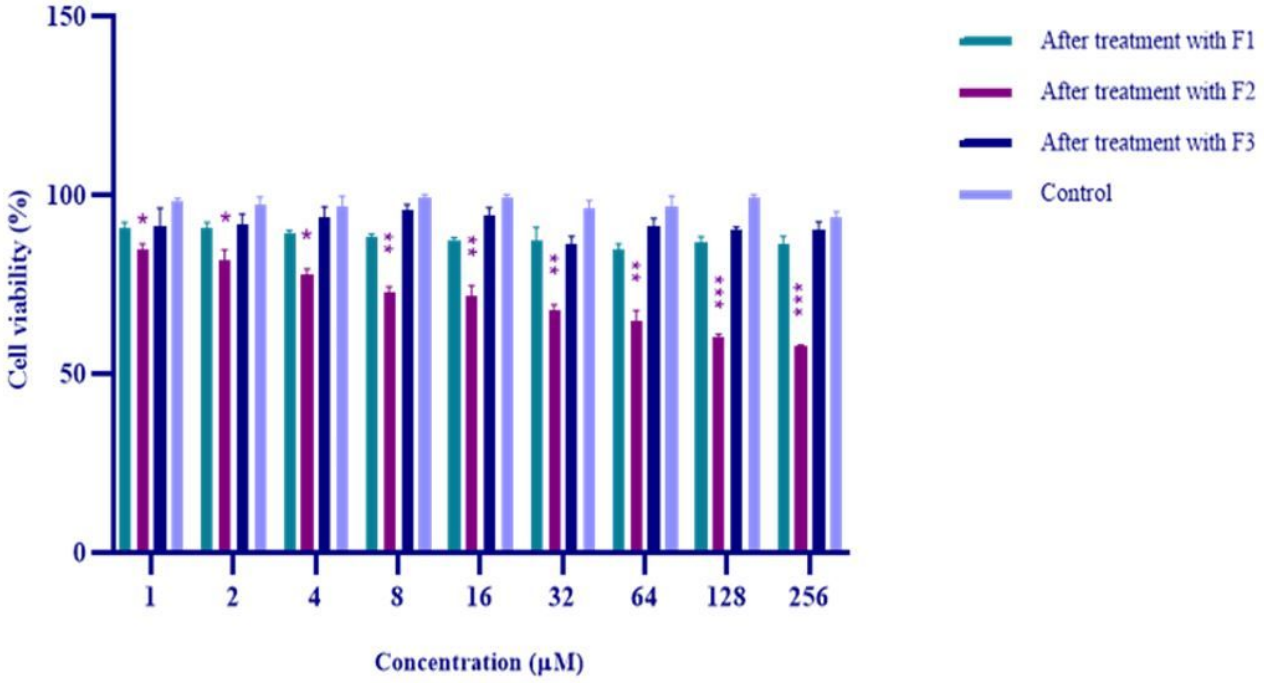

Figure 7

Cell viability percentages of HEK 293 cells treated with ALG/CS-encapsulated *E. angustifolia*, free NPs, and free extract over 24 hours were compared to control and free extract. The outcomes represent the mean and SD of three distinct experiments. The significant values used were ***p<0.001, **p<0.01, *p<0.0.5. F1; Chitosan + Alginate, F2; *E. angustifolia,* F3; *E. angustifolia* + alginate + chitosan.